



Contents lists available at ScienceDirect

Tectonophysics

journal homepage: www.elsevier.com/locate/tecto

Seismotectonic characteristics of the northernmost Longitudinal Valley, eastern Taiwan: Structural development of a vanishing suture

J. Bruce H. Shyu *, Chun-Fu Chen, Yih-Min Wu

Department of Geosciences, National Taiwan University, Taipei, Taiwan, ROC

ARTICLE INFO

Article history:

Received 24 February 2015
 Received in revised form 15 September 2015
 Accepted 23 December 2015
 Available online xxxx

Keywords:

Seismotectonics
 Seismicity
 Focal mechanism
 Meilun fault
 Longitudinal Valley suture

ABSTRACT

The Longitudinal Valley in eastern Taiwan is generally considered as the suture of the collision between the Philippine Sea and the Eurasian plates, and has attracted numerous geologic and seismologic studies. In the northernmost part of the valley, however, constraints on how structures develop as the suture turns into the Ryukyu subduction system offshore are still very limited. Therefore, we analyzed relocated seismicity distributions and focal mechanisms of earthquake sequences, together with tectonic geomorphic investigations to further understand the seismotectonic characteristics of this area. In our seismologic observations, we found two previously unidentified reverse faults in the northernmost part of the Longitudinal Valley suture. One is an E–W striking, south-dipping reverse fault near the Liwu River fan delta, and the other is a N–S striking, east-dipping reverse fault near the eastern Central Range front. Both these structures connect with a detachment at ~10 km deep, and may connect with each other to form a curved structural system. The Meilun fault, a well-known active structure that ruptured in a M7.3 earthquake in October 1951, is not seismically active in the past two decades, and may just be part of a secondary branch of the major structural system. In the northernmost part of the Longitudinal Valley suture, we propose that as the Coastal Range bedrocks subduct northward beneath the Eurasian plate with the Philippine Sea plate, the shallow sediments of the Longitudinal Valley, being a buoyant block, do not subduct, but overthrust northward and westward instead.

© 2016 Elsevier B.V. All rights reserved.

1. Introduction

The island of Taiwan is located at the collisional boundary between the Philippine Sea and the Eurasian plates (e.g., Teng 1987, 1990; Shyu et al. 2005a, and references therein; Fig. 1). In eastern Taiwan, the Longitudinal Valley between the Central Range and the Coastal Range is generally considered as the suture of the collision (e.g., York 1976; Teng 1990; Lee et al. 1998, 2001; Shyu et al. 2005b, 2008, 2011). The Ryukyu subduction system, on the other hand, extends southwestward from offshore eastern Taiwan, and intersects with the northernmost Longitudinal Valley suture. As a result, the area of the northernmost Longitudinal Valley is characterized by frequent earthquakes and complex geologic structures (e.g., Bonilla 1975, 1977; Shyu et al. 2005b).

At the northern end of the Longitudinal Valley suture, a small uplifted tableland, the Meilun Tableland, is present (Fig. 2). This distinctive topographic feature is bounded in its west by the Meilun fault, a well-known active fault in eastern Taiwan (e.g., Central Geological Survey 2010). Rupture of this fault produced a M7.3 earthquake in October 1951 (Hsu 1955, 1962). However, due to the relatively short (~100 years) written history of eastern Taiwan, no other fault is

known to have ruptured historically in the northernmost Longitudinal Valley. Furthermore, there is very little information about tectonic geomorphic features other than the Meilun Tableland. As a result, how the Longitudinal Valley suture terminates to the north and how it relates with the Ryukyu subduction system remain poorly understood.

In order to further understand this structural transition area, we analyzed the seismologic characteristics of the northernmost Longitudinal Valley with new earthquake data. We then combined the seismologic observations with detailed tectonic geomorphic investigations to identify the general seismotectonic characteristics of this area. Such information enabled us to propose a model for the structural evolution of the vanishing suture at the northernmost Longitudinal Valley.

2. Geologic settings of the northernmost Longitudinal Valley

Taiwan, located at the convergent plate boundary between the Philippine Sea plate and the Eurasian plate, is the product of the ongoing collision between the Eurasian continental margin and the Luzon volcanic island arc, part of the Philippine Sea plate (e.g., Teng 1987, 1990; Shyu et al. 2005a, and references therein). The Coastal Range in eastern Taiwan is the collided and attached part of the Luzon volcanic arc. West of the range is the Longitudinal Valley, a linear valley that is generally considered as the suture between the continental basement and the

* Corresponding author. Tel.: +886 2 33669401; fax: +886 2 23636095.
 E-mail address: jbhs@ntu.edu.tw (J.B.H. Shyu).

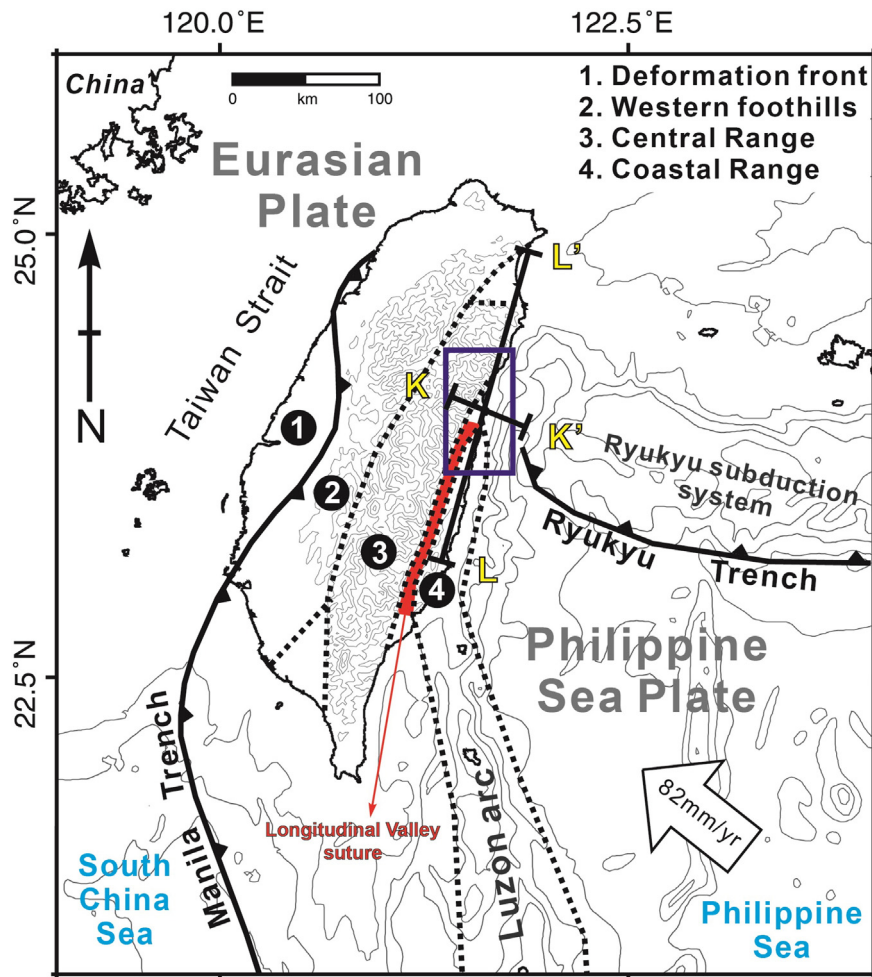


Fig. 1. Tectonic settings of Taiwan and surrounding areas, modified from Shyu et al. (2005a). The dark blue box is the study area. Solid black lines are major structures of Taiwan, and dashed black lines are boundaries of tectonic geomorphic units. The Longitudinal Valley suture is shown in red. K-K' and L-L' are two long seismicity profiles shown in Figs. 5 and 7. The short lines perpendicular to the profile traces represent the projection width of each profile. (For interpretation of the references to color in this figure legend, the reader is referred to the web version of this article.)

collided volcanic arc (e.g., York 1976; Teng 1990; Lee et al. 1998, 2001; Shyu et al. 2005b, 2008, 2011; Fig. 1).

As an active collisional plate boundary, the Coastal Range and the Longitudinal Valley is characterized by high rates of deformation and uplift. For example, many lines of evidence suggest that almost the entire Coastal Range is undergoing rapid uplift. These include the results of recent geodetic measurements (e.g., Ching et al. 2011), the presence of widespread river terraces (e.g., Shyu et al. 2006a), and the existence of multiple steps of marine terraces along the coast east of the Coastal Range (e.g., Liew et al. 1990; Hsieh et al. 2004; Yamaguchi and Ota 2004). The deformation and uplift of the range is likely produced by activities of the Longitudinal Valley fault, which is one of the most active structures of Taiwan and crops out along the western edge of the Coastal Range (e.g., Angelier et al. 1997; Shyu et al. 2005b, 2006a, 2007). Holocene slip rate of the fault can be as high as more than 20 mm/year (e.g., Shyu et al. 2006a; Champenois et al. 2012).

The Coastal Range does not extend to the northern end of the Longitudinal Valley, however. Instead, the northernmost part of the valley is bounded in its east by the Meilun Tableland, an uplifted fluvial/marine terrace with the highest point at ~100 m above sea level (Fig. 2). It is generally believed that the uplift of the tableland is due to the activity of the Meilun fault, which crops out along the western edge of the tableland and ruptured in October 1951 (e.g., Hsu 1962). This M7.3 event is the only historical earthquake involving surface ruptures in this area. According to historical documents, co-seismic vertical offsets across

the rupture were up to ~1.2 m, and left-lateral offsets were up to ~2 m (e.g., Hsu 1955; Bonilla 1975, 1977). Recent geodetic observations, nonetheless, show that no significant strain is accumulating across the fault (e.g., Yen et al. 2011; Chen et al. 2014).

3. Methods

In this study, we analyzed the distribution of relocated earthquake data to identify the structural patterns of the northernmost Longitudinal Valley. We then combined focal mechanisms of different earthquake sequences occurred in the area to further understand the types of structures identified. Our data source is the earthquake catalogue collected by the Central Weather Bureau Seismic Network (CWBSN; Shin 1992, 1993) of Taiwan from January 1991 to December 2010. Considering the relatively sparse station coverage in eastern Taiwan, we used all events that have arrivals recorded by more than four stations. In total, 56,281 events were selected.

We adapted the 3-D location with station correction (3DCOR; Wu et al. 2003, 2008a) as the method to relocate the earthquakes. This method uses the 3-D velocity model of Taiwan (Wu, Y.-M. et al., 2007, 2009). Other than CWBSN, data from Taiwan Strong-Motion Instrumentation Program (TSMIP) stations, Taiwan Integrated Geodynamics Research (TAIGER) stations, and Japan Meteorological Agency (JMA) stations are also utilized in the earthquake relocation processes in order to improve the station coverage (Fig. 3).

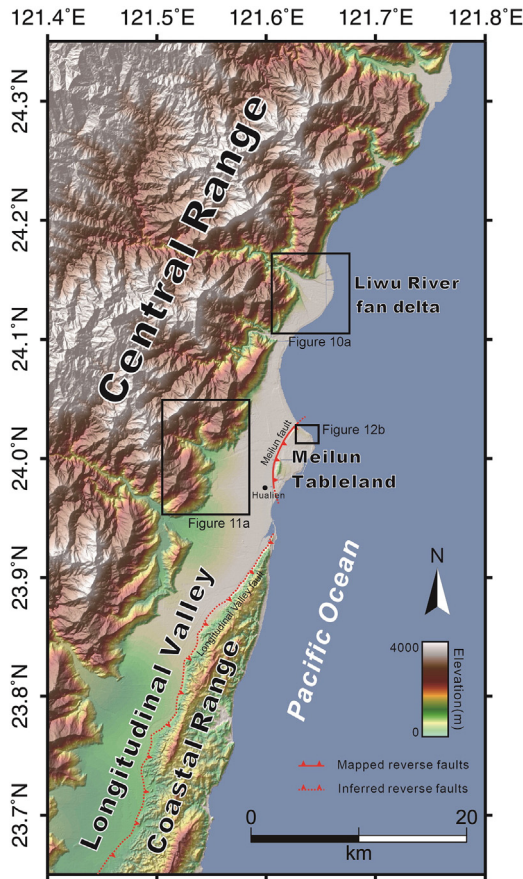


Fig. 2. Geography and mapped major active faults in the study area. The Meilun Tableland and the Liwu River fan delta are two major geographic features investigated in this study. The fault bounding the western edge of the Meilun Tableland is the Meilun fault.

The focal mechanisms of selected earthquakes were determined by a genetic algorithm produced by Wu et al. (2008b). As shown in previous studies (e.g., Kobayashi and Nakanishi 1994; Wu et al. 2008b; Lee et al. 2015), using a genetic algorithm to determine focal mechanism by polarities of P-first motion requires less amount of calculations compared to using grid search methods, and can provide good quality focal mechanism information for the Taiwan area.

In order to obtain more information of the possible active structures identified by seismologic data, we conducted tectonic geomorphic mappings of topographic features using a 40-m resolution digital elevation model (DEM) of the area, augmented by higher resolution air photos and satellite images available from the Google Earth platform. We then performed detailed field investigations and surveys with real-time kinematic (RTK) GPS to look for topographic expressions of the structures mapped.

4. Earthquake distribution and focal mechanisms

4.1. Earthquake relocation results

The results of our earthquake relocation are shown in Fig. 4. In the map view, the seismicity after relocation became clearly closer to each other compared with that before relocation. After the application of 3DCOR earthquake relocation, the RMS of travel time residuals decreased from 0.20 to 0.15 s. The location errors at horizontal (ERH) and depth (ERZ) directions also decreased from 0.44 to 0.40 km, and from 0.59 to 0.41 km, respectively.

In order to identify any possible subsurface structures in the study area, we made several seismicity cross-sections. Along a long E–W striking seismicity profile across the Central Range and the Meilun Tableland (Fig. 5), two previously identified seismicity clusters beneath this region are present (Kuothen et al. 2004). The cluster at about 20 km deep is likely produced by the seismic activity of the Central Range fault beneath the Central Range (#2 in Fig. 5; Kuothen et al. 2004), and the cluster at about 30–40 km deep beneath the coastline and the Meilun Tableland is likely related with the Longitudinal Valley fault (#1 in

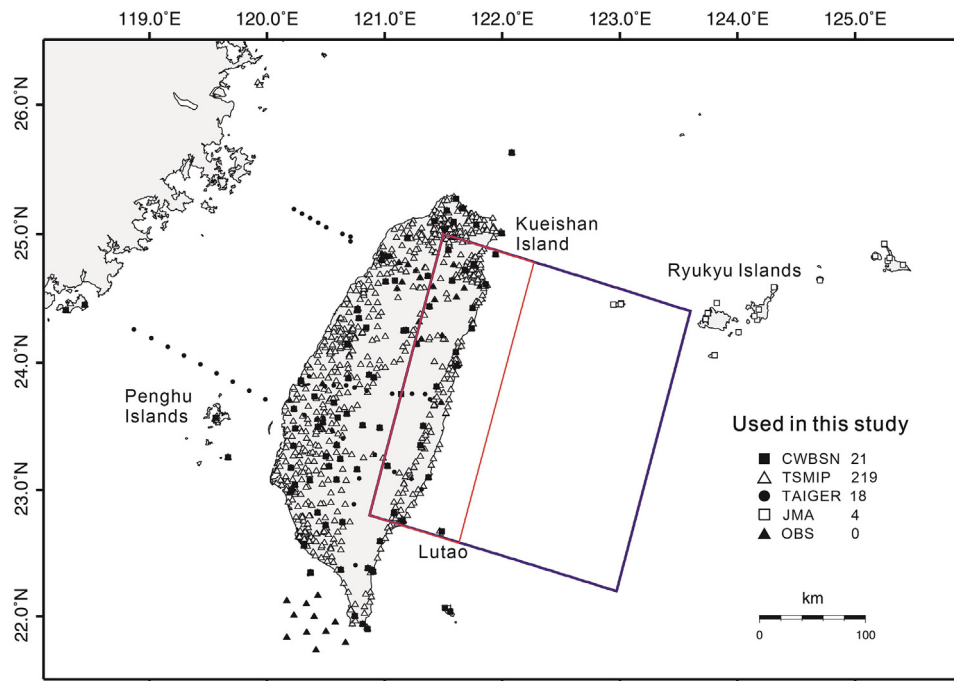


Fig. 3. Distribution of seismic stations used in this study. We have utilized stations from the CWBSN, TSMIP, TAIGER, and JMA networks. The red box shows the area in which earthquake events were selected. The blue box shows the area in which data from seismic stations were used. (For interpretation of the references to color in this figure legend, the reader is referred to the web version of this article.)

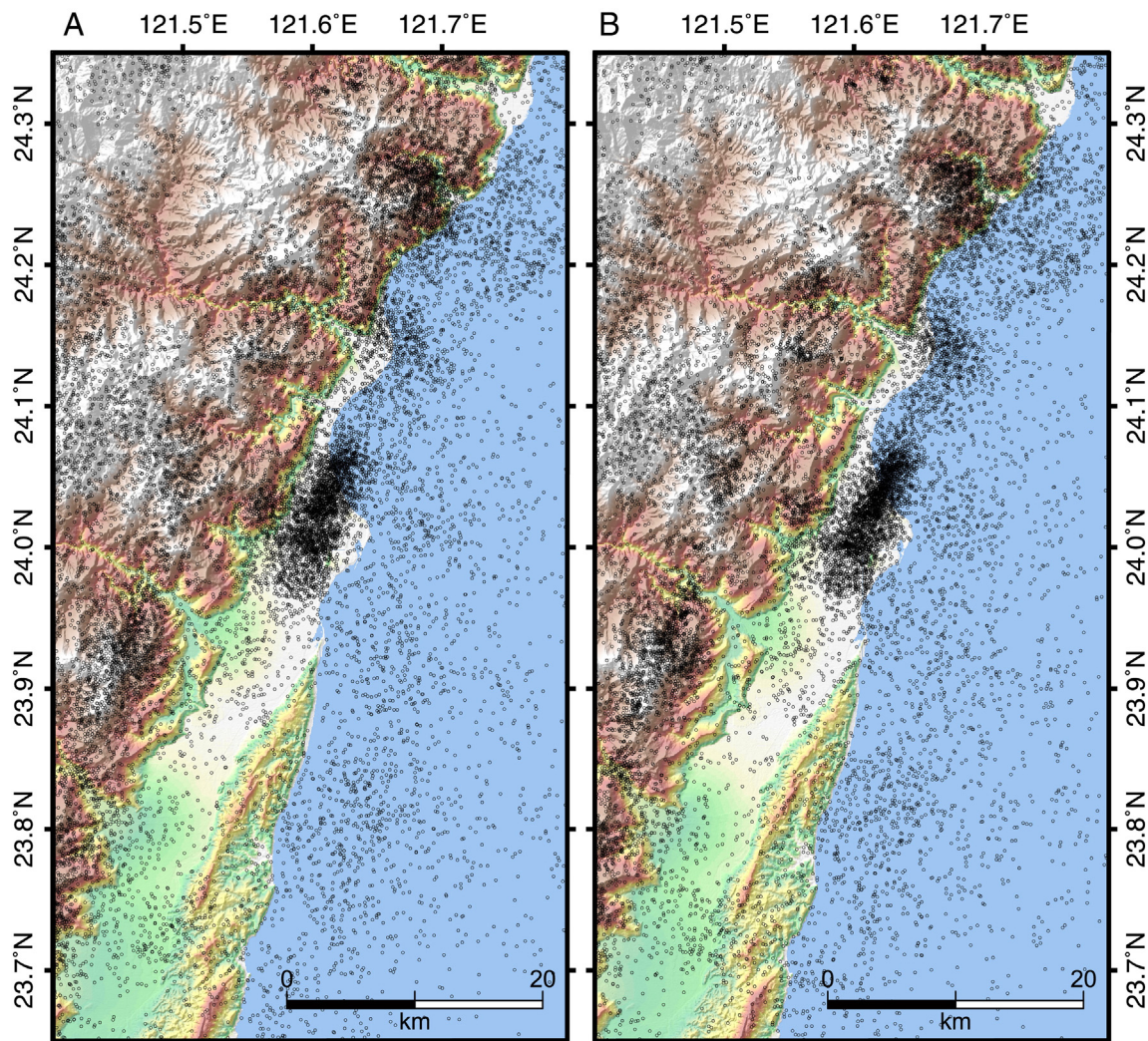


Fig. 4. Distribution of seismicity (A) before and (B) after our relocation. The seismicity after relocation became clearly closer to each other compared with that before relocation.

Fig. 5; Kuo Chen et al. 2004). Other than these two clusters, many earthquakes occurred at about 10 km deep below the Meilun Tableland, and a linear seismicity cluster extends to the surface west of the tableland (#3 in Fig. 5). We infer that this seismicity cluster represents a structure that crops out near the eastern Central Range front. This structure would be different from the Longitudinal Valley fault, since the seismicity clusters are clearly separated at different depths. Moreover, the shallow cluster is only present in the northern Longitudinal Valley, whereas events in the deeper cluster can be traced all the way to the southern part of the valley, as pointed out by Wu, Y.-M. et al. (2009).

In order to further understand the geometry of the seismicity cluster below the Meilun Tableland, we drew a series of E–W seismicity cross-sections in the northernmost Longitudinal Valley (Fig. 6). In these profiles, a clear east-dipping structure is illuminated by the seismicity, and the structure appears to extend to the surface near the eastern Central Range front. This structure is also different from the Meilun fault, since the location where this structure crops out at the surface would be more than 5 km west of the Meilun fault (red line and red arrows in Fig. 6), much more than the relocation error in the horizontal direction. No seismicity is present directly below the Meilun fault, and this suggests that the Meilun fault is not seismically active during the past 20 years.

Several features are visible along a long N–S striking seismicity profile that extends from the northern Central Range to the middle part of the Coastal Range (Fig. 7). Firstly, the Wadati–Benioff zone of

the Ryukyu subduction system is located at about 40 km deep at the southern end of the profile, and gets to about 100 km deep at the northern end of the profile (green dashed line in Fig. 7; Wu, Y.-M. et al., 2009). At about 20 km deep in the southern part of the profile, clear seismic activity of the Longitudinal Valley fault is present, as previously identified by Wu, Y.-M. et al. (2009) and Shyu et al. (2011). These seismic activities can extend to our study area to the seismicity cluster at about 35–40 km deep (yellow dashed line in Fig. 7). The seismicity appears to become deeper from south to north, in a similar pattern as the Wadati–Benioff zone between the Philippine Sea plate and the Eurasian plate. This indicates that the northern Coastal Range may be subducting northward beneath the Eurasian plate together with the Philippine Sea plate, as proposed in several previous studies (F. T. Wu et al., 2009; Huang et al. 2012).

The seismicity at about 10 km deep below the Meilun Tableland, however, shows a different geometry. After a gentle northward deepening trend that is similar to the two seismicity groups mentioned above, this cluster appears to extend to the surface in a listric pattern near the Liwu River fan delta, north of the Meilun Tableland (red dashed box in Fig. 7). We propose that this cluster represents an E–W striking structure that dips to the south and crops out near the Liwu River fan delta. We made two additional N–S seismicity profiles that focus on the northernmost Longitudinal Valley (Fig. 8). Along the profile across the northern Coastal Range, the Meilun Tableland, and the Liwu River fan delta, the seismicity cluster identified above (#1) appears to separate from

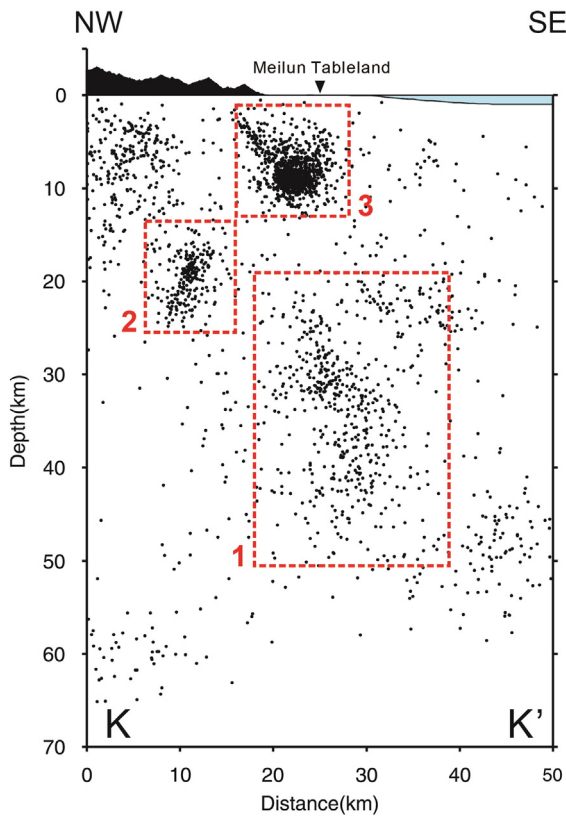


Fig. 5. A long E–W seismicity profile across the study area. The #2 seismicity cluster at about 20 km deep is likely produced by the seismic activity of the Central Range fault beneath the Central Range, and the #1 cluster at about 30–40 km deep is likely related with the Longitudinal Valley fault. Other than these two clusters, many earthquakes (cluster #3) occurred at about 10 km deep below the Meilun Tableland. The location of the profile is shown in Fig. 1.

other seismicity (#2) further to the north, and illuminates a structure that crops out near the Liwu River fan delta. Similar pattern is also visible along the profile further offshore.

4.2. Earthquake sequences and focal mechanisms

From the observations of the seismicity distribution of the northernmost Longitudinal Valley area, we found that besides the known Longitudinal Valley fault and the Meilun fault, there may be two more previously unidentified structures in the area. One appears to be an east-dipping structure that may crop out near the eastern Central Range front; the other appears to be an E–W striking, south-dipping structure that may crop out near the Liwu River fan delta. In order to further understand these two proposed structures, we sought for earthquake sequences that occurred near these areas to obtain more seismologic information. We applied the method of spatiotemporal double-link cluster analysis to identify earthquake sequences in the catalogue. This method is similar to the single-link cluster analysis proposed by Davis and Frohlich (1991), and with temporal and spatial linking parameters of 3 days and 5 km, respectively. These parameters were usually used for declustering the CWBSN catalogue (e.g., Wu and Chiao 2006; Wu and Chen 2007) or identifying aftershocks in an earthquake sequence (e.g., Wu and Chiao 2006; Lee et al. 2015).

Three earthquake sequences were found in this study. Due to the small magnitudes of the mainshocks, all three sequences lasted only a few days. The first one is related with a M_L 4.7 event occurred on 19 December 2009, beneath the northern part of the Coastal Range, and consists of ~150 events. In this sequence, most of the events occurred at depths between 20 and 40 km, with mostly reverse faulting focal mechanisms (Fig. 9A). Therefore, this sequence is likely produced

by the activity of the northern Longitudinal Valley fault. No event occurred shallower than 10 km. This is consistent with our hypothesis that the Longitudinal Valley fault system and the structures at 10 km deep beneath the Meilun Tableland are two different systems.

The earthquake sequence related with a M_L 4.4 event on 30 April 2005 beneath the Meilun Tableland reveals much more information about the structure (Fig. 9B). This sequence has about 400 events. Similar to the #3 seismicity cluster in Fig. 5, most of the earthquakes of this sequence occurred at depths about 10 km, with shallower events illuminating the east-dipping structure that may crop out near the eastern Central Range front. The focal mechanisms of earthquakes in the sequence, however, are quite complex. We therefore made two seismicity profiles of this sequence, one perpendicular and one parallel to the trend of the Longitudinal Valley. Along the one perpendicular to the trend of the valley, we found that the events that occurred on the proposed east-dipping structure were mostly reverse faulting event. Along the profile parallel to the trend of the valley, we observed that the seismicity cluster at about 10 km deep appears to form a detachment, with the materials below moving northward. Some previous models (e.g., Chen et al. 2014) propose that Central Range rocks form the basement of the entire Longitudinal Valley. However, we suggest that the valley should be underlain by Coastal Range materials at least in its eastern part, since the Central Range fault would constitute a major boundary between Central Range rocks and the Longitudinal Valley sediments (e.g., Kuo Chen et al. 2004; Shyu et al. 2006b; Lee et al. 2014). Therefore, the deeper materials beneath the 10-km-deep detachment are likely the Coastal Range materials that appear to be subducting northward. If so, this detachment would represent the boundary between the subducting Coastal Range materials and the shallow Longitudinal Valley sediments that are too buoyant to subduct.

Few larger earthquakes occurred in the northern part of the study area. The largest one was a M_L 4.3 event that occurred on 28 September 2010 (Fig. 9C). In this earthquake sequence there were only about 40 aftershocks, and most of them were quite small, thus we were unable to obtain many focal mechanisms of the events. Nonetheless, from the distribution of the aftershocks, it is quite clear that the events illuminated a south-dipping structure that may crop out north of the Liwu River fan delta. The focal mechanisms are mostly reverse faulting, with minor right-lateral motion.

5. Geomorphic evidence for the proposed structures

In our seismologic observations, two previously unidentified structures were proposed in the study area. Both structures appear to connect with the detachment identified by the seismic cluster at about 10 km deep, as discussed above. An E–W striking, south-dipping reverse fault may crop out near the Liwu River fan delta, and the other is a N–S striking, east-dipping reverse fault that may crop out near the eastern Central Range front. Since the study area is mostly overlain by recent fluvial sediments, it is not easy to observe tectonic geomorphic features related with these two proposed structures. Therefore, we decided to focus on the two locations where the faults may crop out and conduct detailed field surveys, in the hope to find potential surface expression of the structures.

5.1. Deformations of the Liwu River fan delta

The Liwu River fan delta, located at the Liwu River mouth, can be separated into three levels of terraces by their elevations (Fig. 10A). According to previous investigations, these three levels of terraces were produced by large-scale paleo-flood events, likely related with breakage of large landslide dams in the upper stream of the Liwu River (Liu 1989). If we assume that the terraces were formed by such events, they would be the remnant of three fans that should be radially symmetrical from the river outlet. To test this, we surveyed the surface of the three terraces in the field using RTK-GPS. The survey was done along a profile

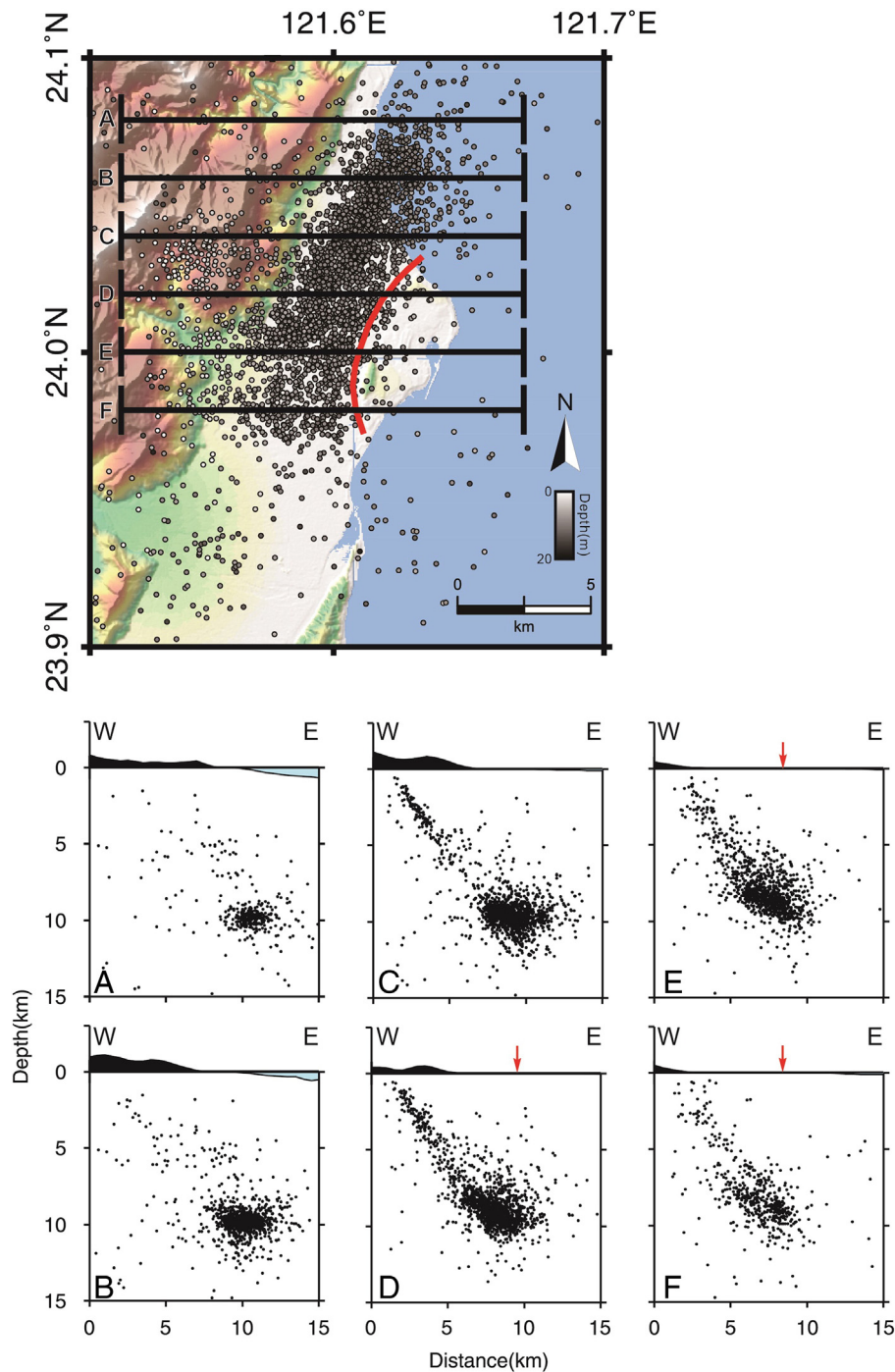


Fig. 6. A series of short E–W seismicity profiles across the northernmost Longitudinal Valley. The short lines perpendicular to the profile traces represent the projection width of each profile. A clear east-dipping structure is illuminated by the seismicity, especially along profiles C–F, and the structure appears to extend to the surface near the eastern Central Range front. This structure is different from the Meilun fault (shown as the red line in map view and red arrows in profiles), since the location it crops out at the surface would be more than 5 km west of the Meilun fault. No seismicity is present directly below the Meilun fault. (For interpretation of the references to color in this figure legend, the reader is referred to the web version of this article.)

line that is parallel to the mountain front trend and perpendicular to the middle axis of the fan, made by extending the Liwu River course outward (light gray bar in Fig. 10A). We then attempted to use simple cosine functions to fit the topographic profile (Fig. 10B). To our surprise, the highest level of the fan delta terraces is not symmetrical on both sides of the middle axis (light gray bar in Fig. 10B), with its southern part higher than its northern part.

This phenomenon may have resulted from many different reasons. A different choice of the middle axis of the fan delta, for example, would explain the apparent asymmetry. But if we try to make the two parts

of the terrace symmetrical, the middle axis would need to locate farther south, away from the outlet of the river and its current riverbed (dark gray bar in Fig. 10A and B). Alternatively, coastal erosion and longshore transport of sediments may have moved the materials of the fan delta. We did, in fact, observe some coastal erosion at the northern part of the profile, where the foot of the fan has been cut to form a sea cliff (Fig. 10B). This, however, would indicate that the area of the terrace's northern part was larger than it is now, and would make moving the middle axis farther south more inappropriate. Therefore, we suggest that the asymmetry of the Liwu River fan delta terrace may represent

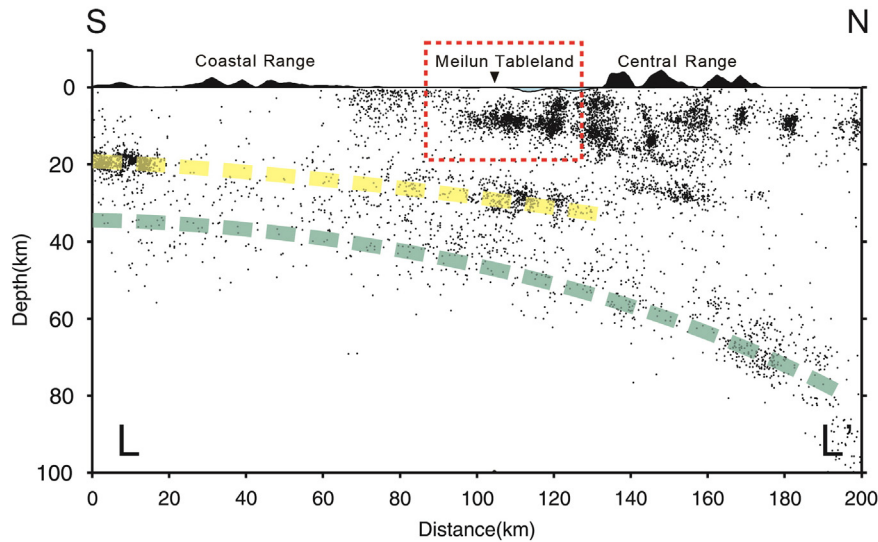


Fig. 7. A long N–S seismicity profile across the study area. The green dashed line shows the Wadati–Benioff zone between the Philippine Sea plate and the Eurasian plate, from about 40 km deep at the southern end of the profile to about 100 km deep at the northern end of the profile. The yellow dashed line shows the seismic activity of the Longitudinal Valley fault, at about 20 km deep in the southern part of the profile and extending to our study area to the seismicity cluster at about 35–40 km deep. The seismicity cluster at about 10 km deep below the Meilun Tableland shows a different geometry, extending to the north at similar depth then to the surface in a listric pattern near the Liwu River fan delta north of the Meilun Tableland (in the red dashed box). The location of the profile is shown in Fig. 1. (For interpretation of the references to color in this figure legend, the reader is referred to the web version of this article.)

a northward tilting deformation. One may argue that this deformation may have been produced by the subsidence of the northern Longitudinal Valley related to the Ryukyu subduction. However, such deformation would have a very large spatial scale, probably many tens of kilometers in length as shown by the distribution of seismicity in

Fig. 7. The apparent deformation of the Liwu River fan delta, nonetheless, occurs within only a few kilometers in length. Therefore, we suggest that the northward tilting is produced by long-term deformation of a south-dipping blind reverse fault, as proposed in our seismicity observations.

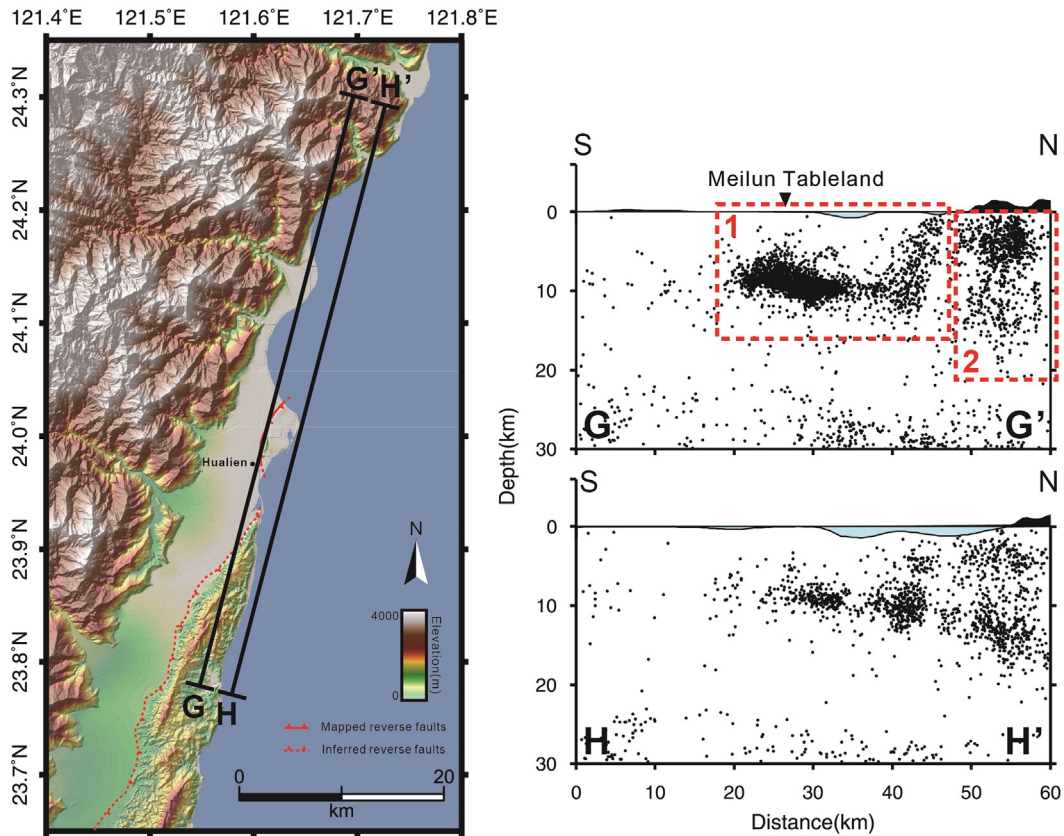


Fig. 8. Two short N–S seismicity profiles across the northernmost Longitudinal Valley. The projection widths of the profiles are shown as the short lines perpendicular to the profile traces. Along the G–G' profile, the seismicity cluster beneath the Meilun Tableland appears to separate from other seismicity further to the north, and illuminates a structure that crops out near the Liwu River fan delta. Similar pattern is also visible along the H–H' profile further offshore.

It is noteworthy that such phenomenon is only visible on the highest fan terrace, although the data points are much fewer for the lower terraces (Fig. 10B). Although there is currently no age

constraint on these terraces, the highest terrace is likely older than the lower terraces judging from their occurrences. We therefore suspect that due to the older age of the highest terrace, only this

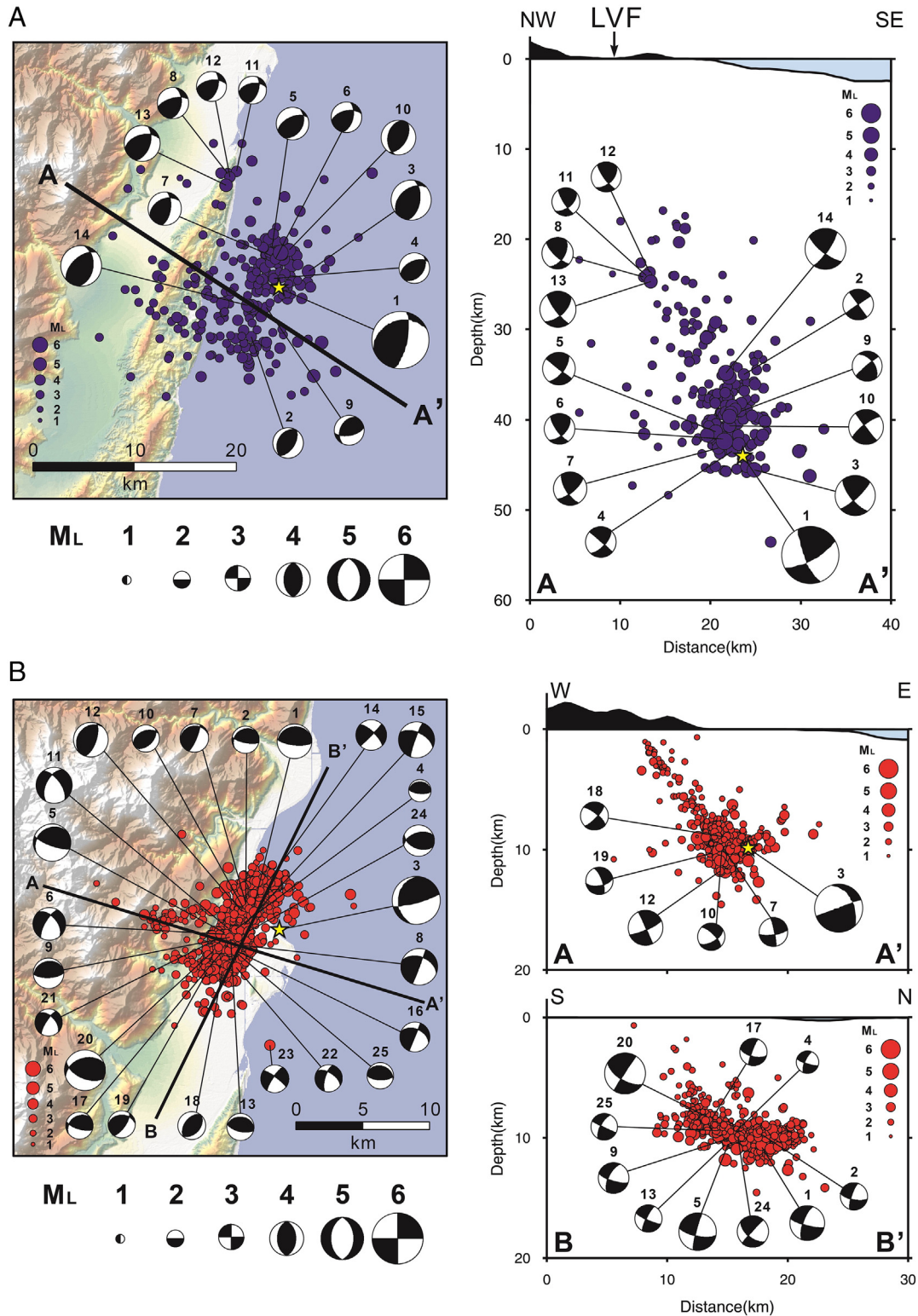


Fig. 9. Three selected earthquake sequences occurred in our study area. (A) The earthquake sequence related with a M_L 4.7 event on 19 December 2009 (shown by the yellow star) beneath the northern part of the Coastal Range. In this sequence, most of the events occurred at depths between 20 and 40 km, with mostly reverse faulting focal mechanisms. (B) The earthquake sequence related with a M_L 4.4 event on 30 April 2005 (shown by the yellow star) beneath the Meilun Tableland. Most of the earthquakes of this sequence occurred at a depth about 10 km, with shallower events illuminating the east-dipping structure that may crop out near the eastern Central Range front. The focal mechanisms of earthquakes in the sequence are quite complex. (C) The earthquake sequence related with a M_L 4.3 event on 28 September 2010 (shown by the yellow star) beneath the Liwu River fan delta. The earthquakes illuminated a south-dipping structure that may crop out north of the Liwu River fan delta, and the focal mechanisms are mostly reverse faulting with minor right-lateral motion. The width of each profile is 10 km. (For interpretation of the references to color in this figure legend, the reader is referred to the web version of this article.)

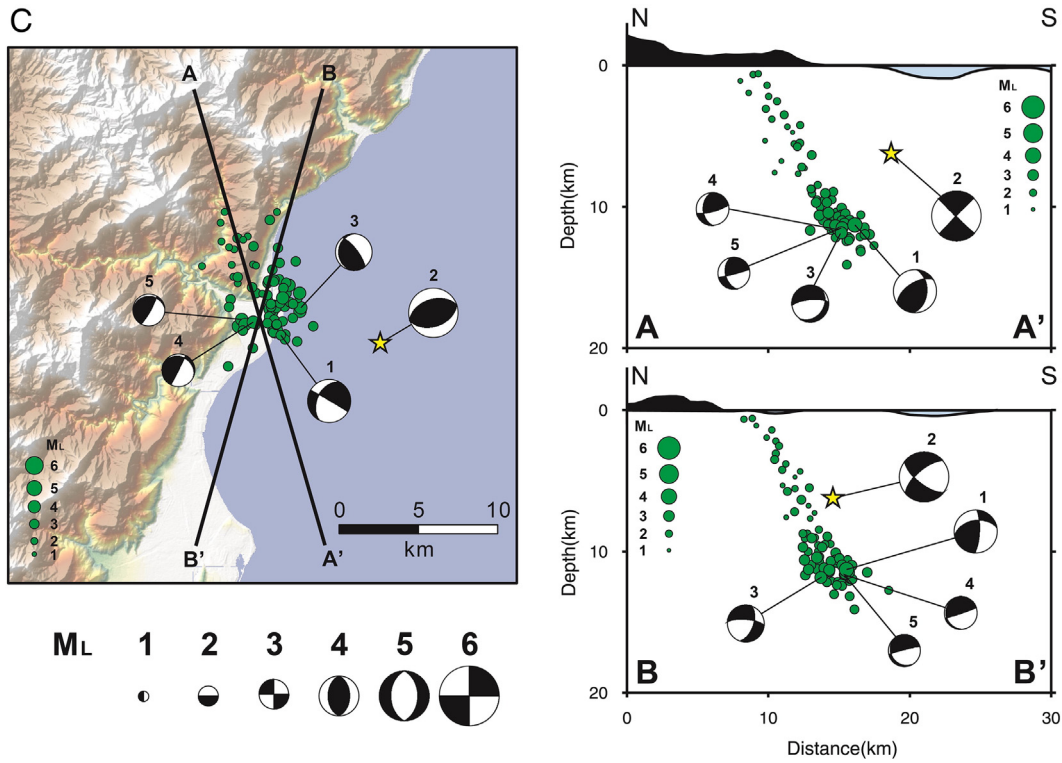


Fig. 9 (continued).

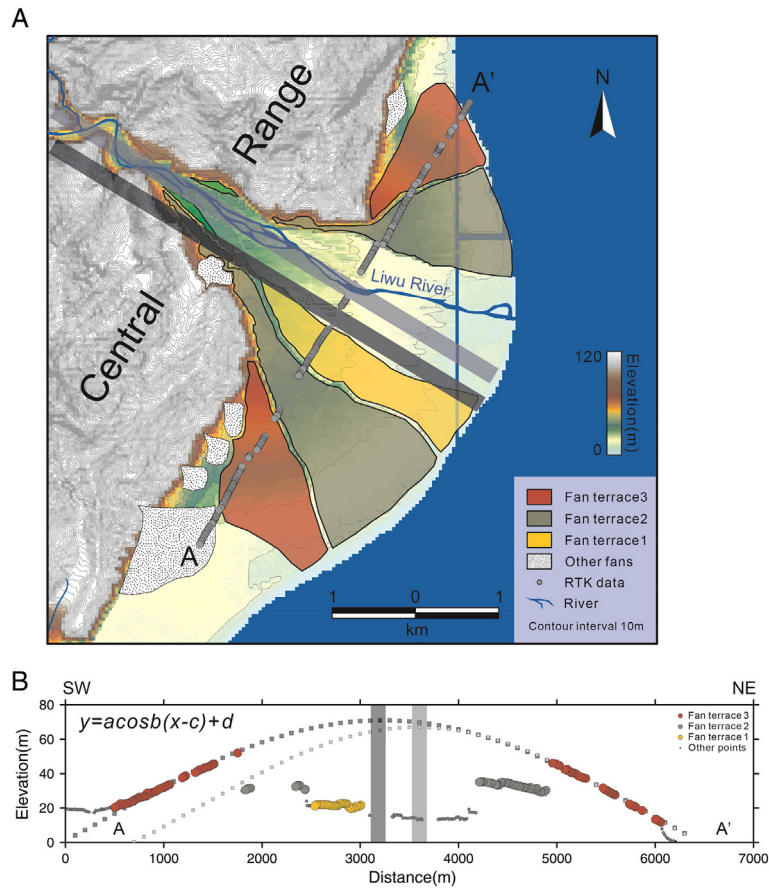


Fig. 10. Results of our tectonic geomorphic mapping and survey in the Liwu River fan delta area. (A) The Liwu River fan delta can be separated into three levels of terraces by their elevations. We surveyed the surface of the three terraces in the field using RTK-GPS along the A-A' profile line that is parallel to the mountain front trend and perpendicular to the middle axis of the fan, made by extending the Liwu River course outward (shown by the light gray bar). (B) We attempted to use simple cosine functions to fit the topographic profile. The highest level of the fan delta terraces appears not symmetrical on both sides of the middle axis (light gray bar), with its southern part higher than its northern part. If we try to make the two parts of the terrace symmetrical, the middle axis would need to locate farther south (dark gray bar), away from the outlet of the river and its current riverbed.

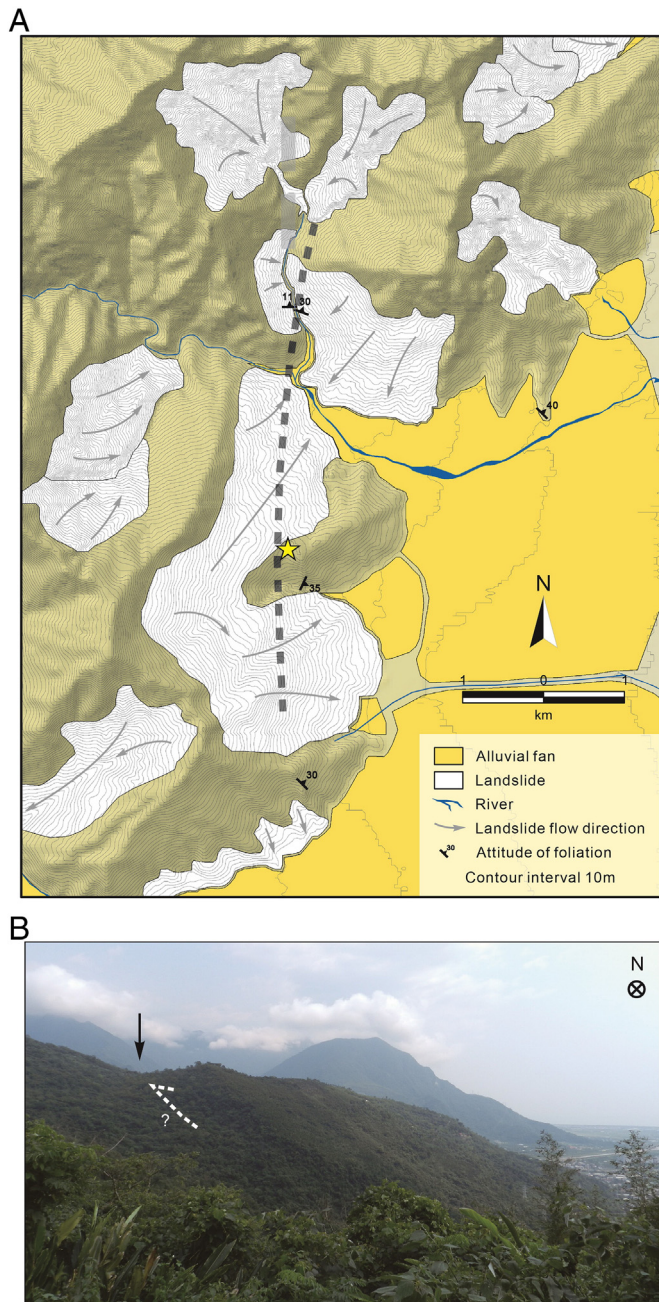


Fig. 11. Results of our tectonic geomorphic mapping and field investigation at the eastern flank of the Central Range. (A) This area is covered by many landslides and their deposits, which are the sediment sources of the many recent alluvial fans. (B) A peculiar west-facing scarp cutting across a ridge on the eastern flank of the Central Range is present approximately at the location where the inferred east-dipping fault would crop out (shown by the gray dashed line in (a)). The photo was taken at the yellow star in (a). (For interpretation of the references to color in this figure legend, the reader is referred to the web version of this article.)

terrace could accumulate enough deformation to show the asymmetrical pattern.

5.2. Bedrock patterns in the eastern Central Range flank

For the proposed east-dipping structure near the eastern Central Range front, related topographic features are even harder to find. After mapping this area using a 40-m resolution DEM and Google

Earth images, we found that this part of the Central Range is covered by numerous landslides and their deposits, which are the sediment sources of the many recent alluvial fans covering the low-lying part of this area (Fig. 11A). Due to the widespread landslides, it is quite difficult to find bedrock outcrops in this area. We did, however, find a broken ridge line that appears to be east-side up on the eastern flank of the Central Range, approximately at the location where the inferred east-dipping fault would crop out (Fig. 11B). The existence of such a broken ridge line, with an apparent east-side upward structure, is quite peculiar and may be related to the proposed structure. We also attempted to measure the bedding attitudes of the bedrock at the limited outcrops, but the data do not show any consistent trend (Fig. 11A). Therefore, even if the broken ridge line indeed represents the location of the inferred fault, we are unable to extend its location to the north or south based on surface observations.

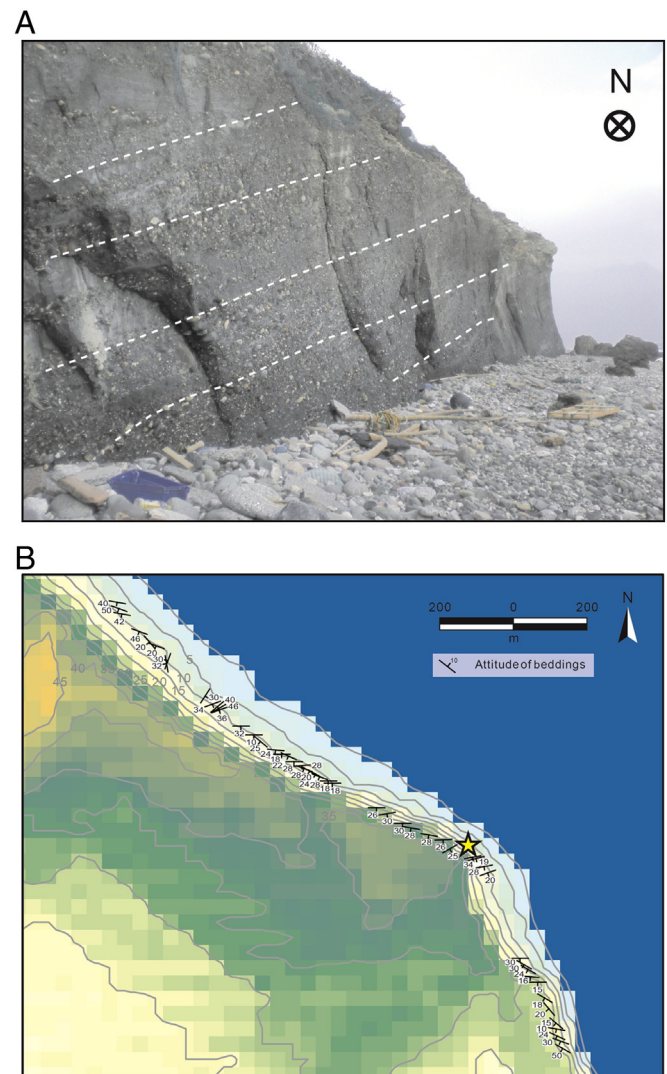


Fig. 12. Bedrock outcrop along the northern edge of the Meilun Tableland and the bedding attitude measurement results. (A) Along the northern edge of the Meilun Tableland, continuous outcrops of the underlying bedrocks are present due to coastal erosion. Interbedded gravels and sands are clearly visible in the outcrops (shown by the white dashed lines). The photo was taken at the yellow star in (B). (B) Our bedding attitude measurements revealed that the bedrock layers are E–W striking and dip to the south. (For interpretation of the references to color in this figure legend, the reader is referred to the web version of this article.)

6. Discussion

6.1. The Meilun fault and the Meilun Tableland

Since the Meilun fault ruptured in the October 1951 earthquake, the fault has long been identified as one of the major active faults in eastern Taiwan (e.g., Central Geological Survey 2010). Up to ~1.2 m of coseismic vertical offsets and up to ~2 m of sinistral offsets were reported in historical documents during the 1951 event (e.g., Hsu 1955; Bonilla 1975, 1977). The onland length of the fault, however, is less than 10 km. This length appears to be too short considering the earthquake had a magnitude of 7.3 (Hsu 1962). Therefore, some suggest that the fault should extend further offshore to the north (e.g., Shyu et al. 2005b).

Since we did not observe any seismic activity on the Meilun fault in our relocated seismicity, we began to wonder the role the fault plays in the study area. Because the Meilun faults bound the western edge of the Meilun Tableland, if the formation of the tableland is in fact due to the movement along the fault, such a long-term accumulated deformation would suggest that the fault is the major structure of the area, albeit its recent seismic quiescence. Therefore, we investigated the tableland in the field to see if its long-term deformation is produced by the Meilun fault.

The Meilun Tableland is located in the suburb of the Hualien City and has been densely developed. Thus it was not easy to observe the sediment layers underlying the tableland surface. However, along the northern edge of the tableland, continuous outcrops of the underlying bedrocks are present due to coastal erosion (Fig. 12A). There, we found that the bedrock layers are E–W striking and dip to the south (Fig. 12B). Such deformation patterns are unlikely to have produced the left-lateral and reverse motion on the NE–SW striking Meilun fault at the western edge of the tableland. Therefore, we propose that there is an E–W striking reverse fault north of Meilun Tableland offshore, whose activity produced the uplift and deformation of the tableland. Judging from its geometrical pattern, this fault may connect with the Meilun fault somewhere offshore, and may not necessarily be the same fault as the E–W striking reverse fault we observed in the seismicity distribution near the Liwu River fan delta. If so, this E–W striking reverse fault was not seismically active in the past two decades, just like the Meilun fault. These two E–W striking structures, however, are likely related, possibly connected by the same detachment at ~10 km deep.

6.2. Proposed structural model for the northernmost Longitudinal Valley suture

Our analysis of relocated seismic data and field investigations suggests that there are two previously unidentified reverse faults in the northernmost part of the Longitudinal Valley suture. These two structures are the E–W striking, south-dipping reverse fault near the Liwu River fan delta, and the N–S striking, east-dipping reverse fault near the eastern Central Range front. Both faults appear to connect to a detachment beneath the northernmost Longitudinal Valley at a depth of about 10 km. Thus we believe that these two faults may connect with each other at the surface, forming a curved reverse fault system as shown in Fig. 13. We suggest that this structural system is different from the Longitudinal Valley fault system, since seismicity distributions of the two systems are clearly separated. The Meilun fault, a well-known active structure in this area, does not seem to be active seismically in the past two decades, neither the long-term deformation of the Meilun Tableland produced by the activity of the fault. Instead, there may be another E–W striking reverse fault offshore north of the Meilun Tableland that is responsible for the uplift and formation of the tableland. As we discussed above, this structure may connect with the Meilun fault. In such case, we hypothesize that both structures branch out from the detachment at 10 km deep.

The curved reverse fault system may therefore be the actual major structural system at the northernmost Longitudinal Valley. Such a system would be able to absorb the northwestward convergence between the Coastal Range and the Central Range, and has been proposed by sandbox models of the northernmost Longitudinal Valley (e.g., Lu and Malavieille 1994). We tested this hypothesis by comparing our seismologic observations with tomographic results of eastern Taiwan (Wu et al. 2007; Fig. 14). The results show that the structural system we proposed, from the detachment at ~10 km deep to the south-dipping reverse fault near the Liwu River fan delta, is approximately coincident with a boundary between low Vp and high Vp/Vs materials above and high Vp and low Vp/Vs materials below. Therefore, we suggest that the detachment forms the boundary between the shallow Longitudinal Valley sediments and the deeper Coastal Range bedrocks.

Based on these observations and interpretations, we propose a structural development model for the study area (Fig. 15). In the northernmost part of the Longitudinal Valley suture, as the Coastal Range rocks subduct northward beneath the Eurasian plate together with the Philippine Sea plate, the shallow sediments of the Longitudinal Valley become a buoyant block and do not subduct. As a result, a detachment forms between the sediments and the bedrocks, and the shallow Longitudinal Valley sediments overthrust northward and westward instead, forming the curved reverse fault system. This system consists of the two previously unidentified reverse faults, and is different from the Longitudinal Valley fault system that is much deeper. Although the N–S striking reverse fault identified in this study appears to break the

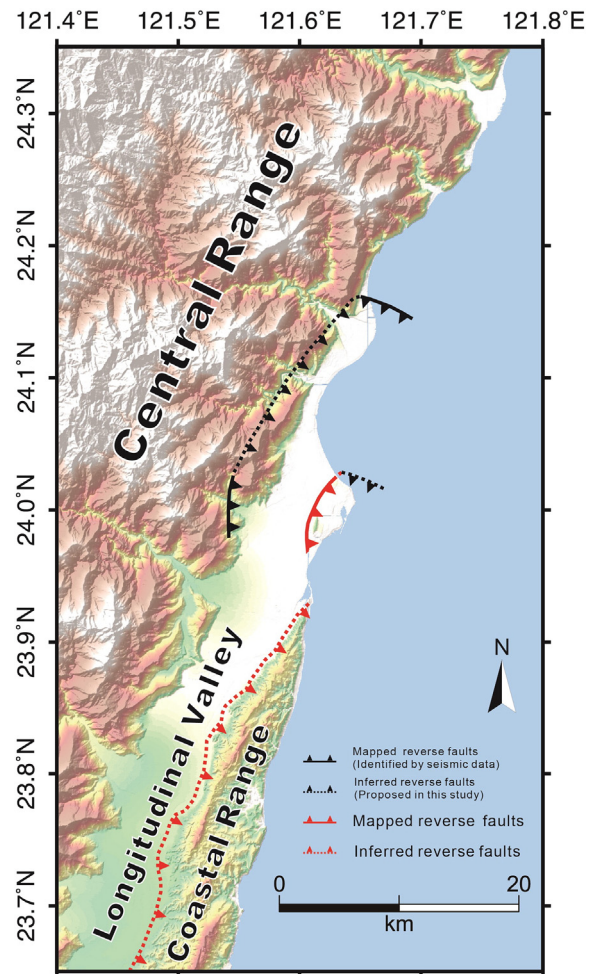


Fig. 13. Proposed connection of the two reverse faults identified in this study. The two faults identified in this study (shown by solid black lines) may connect with each other at the surface, forming a curved reverse fault system.

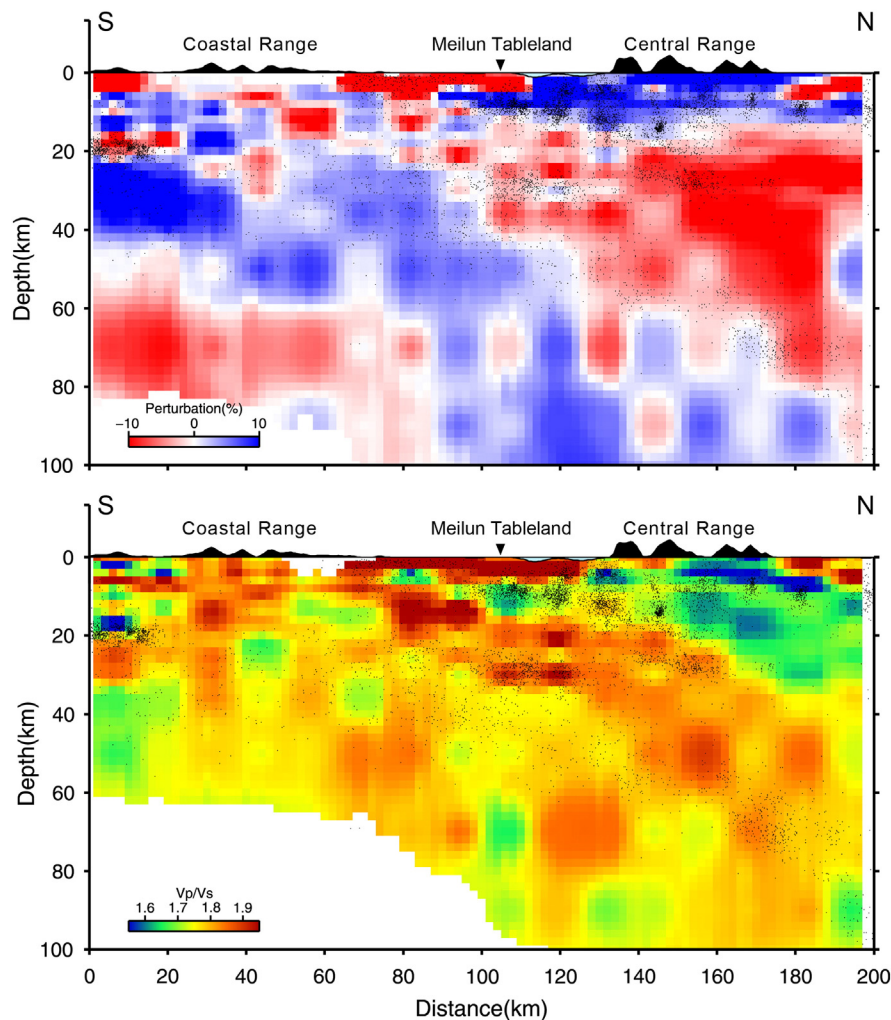


Fig. 14. Tomographic results in eastern Taiwan, showing that the detachment at ~ 10 km deep beneath the Meilun Tableland identified in this study forms the boundary between low V_p and high V_p/V_s materials above and high V_p and low V_p/V_s materials below. The tomographic data were obtained from Wu et al. (2007), and the cross-section line is following line L-L' shown in Fig. 1.

westernmost Central Range, we suggest that this fault forms the boundary between the Central Range metamorphic rocks and the shallow sediments of the Longitudinal Valley. Due to the irregular shape of the eastern Central Range mountain front, this fault would occasionally cut through a small piece of the easternmost Central Range. A similar phenomenon has also been identified near the southernmost part of the Longitudinal Valley (Shyu et al. 2008). The Meilun fault and another E–W striking reverse fault offshore north of the Meilun Tableland, which was active in producing the October 1951 earthquake, would therefore be a secondary branching system of this major system.

On the basis of decadal geodetic observations such as GPS and InSAR analyses, it has been proposed that the crustal block of the Hualien area, including the Meilun Tableland, is moving northeastward (e.g., Yen et al. 2011; Chen et al. 2014). This movement has been interpreted to relate to tectonic escape of the northernmost Longitudinal Valley (Chen et al. 2014). Such observations would be consistent with the proposed structural model based on our seismological and geomorphic analyses (Fig. 15). In our model, however, the northward motion of the northernmost Longitudinal Valley block is related to the northward subduction of the Philippine Sea plate, and the buoyancy of the shallow Longitudinal Valley sediment makes it eventually detached from the downgoing plate, creating the detachment below the Meilun Tableland area at about 10 km deep. Our model provides a better interpretation for the apparent long-term deformation patterns of the gravel beds underlying the Meilun Tableland, whereas a tectonic escape model would be

difficult to interpret such deformation patterns. Furthermore, little surface deformation of the Meilun fault was observed in the geodetic analyses (Yen et al. 2011; Chen et al. 2014), consistent with our proposition that the fault may be a secondary branching system of the major structural system in the area.

7. Conclusions

In order to understand the structural development at the northernmost Longitudinal Valley suture, we analyzed relocated seismicity distributions and focal mechanisms of selected earthquake sequences, as well as conducted field surveys to search for surface expressions of potential structures. In our seismologic observations, we found two previously unidentified reverse faults that are illuminated by seismicity in the study area. These two structures are: (1) an E–W striking, south-dipping reverse fault near the Liwu River fan delta; and (2) a N–S striking, east-dipping reverse fault near the eastern Central Range front. Both these structures connect with a detachment at ~ 10 km deep, and may connect with each other to form a curved structural system. This structural system would be different from the Longitudinal Valley fault system, since the latter is likely much deeper according to our seismological analysis.

We did not see any seismic activity of the Meilun fault in the past two decades. Furthermore, the long-term deformation of the Meilun Tableland does not seem to be produced by the activity of the Meilun fault.

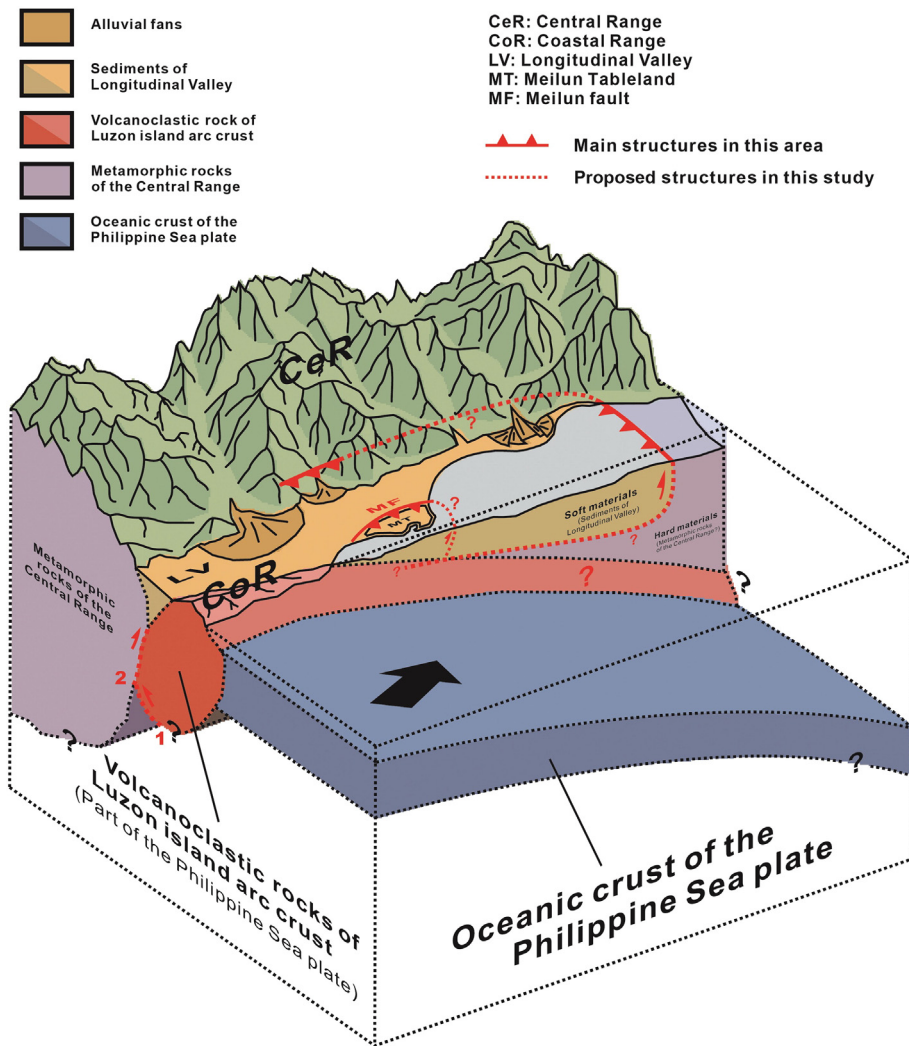


Fig. 15. Proposed structural development model for the northernmost Longitudinal Valley suture in eastern Taiwan. As the Coastal Range bedrocks subduct northward beneath the Eurasian plate with the Philippine Sea plate, a detachment forms between the sediments and the bedrocks, and the shallow Longitudinal Valley sediments overthrust northward and westward instead, forming the curved reverse fault system. This system consists of the two previously unidentified reverse faults. The Meilun fault and another E–W striking reverse fault offshore north of the Meilun Tableland is likely a secondary branching system of this major system. 1: Proposed Longitudinal Valley fault seismic activity illuminated by the seismicity cluster #1 shown in Fig. 5; 2: proposed Central Range fault seismic activity illuminated by the seismicity cluster #2 shown in Fig. 5.

Instead, another E–W striking reverse fault offshore north of the Meilun Tableland may be responsible for the uplift and deformation of the tableland. This fault would connect with the Meilun fault, forming a secondary branching system of the major structural system of the area.

In our proposed structural development model for the northernmost Longitudinal Valley suture, as the Coastal Range bedrocks subduct northward beneath the Eurasian plate together with the Philippine Sea plate, the shallow Longitudinal Valley sediments form a buoyant block and do not subduct. Therefore, a detachment develops between the shallow sediments and the Coastal Range bedrocks, and the sediments overthrust northward and westward instead.

Acknowledgments

We have benefited greatly from discussions with C.-H. Chang, C.-P. Chang, W.-A. Chao, H.-H. Huang, Y.-S. Lin and J.-Y. Yen. Field investigations and surveys were significantly assisted by Y.-W. Chen, Y.-R. Chuang, C.-Y. Tsai and C.-C. Wang. We especially want to thank the Central Weather Bureau of Taiwan for providing seismic data used in this study. Comments and suggestions from two anonymous reviewers significantly improved this manuscript. This research was supported by

the Ministry of Science and Technology (MOST) of Taiwan (Project 102-2628-M-002-007-MY3 to J.B.H.S.).

References

- Angelier, J., Chu, H.-T., Lee, J.-C., 1997. Shear concentration in a collision zone: kinematics of the Chihshang Fault as revealed by outcrop-scale quantification of active faulting, Longitudinal Valley, eastern Taiwan. *Tectonophysics* 274, 117–143.
- Bonilla, M.G., 1975. A Review of Recently Active Faults in Taiwan. Open File Rep (75–41, 58 pp.) U. S. Geol. Surv., Menlo Park, Calif.
- Bonilla, M.G., 1977. Summary of Quaternary faulting and elevation changes in Taiwan. *Mem. Geol. Soc. China* 2, 43–55.
- Central Geological Survey, 2010. Active Fault Map of Taiwan. Central Geological Survey, MOEA, Taipei.
- Champenois, J., Fruneau, B., Pathier, E., Deffontaines, B., Lin, K.-C., Hu, J.-C., 2012. Monitoring of active tectonic deformations in the Longitudinal Valley (Eastern Taiwan) using Persistent Scatterer InSAR method with ALOS PALSAR data. *Earth Planet. Sci. Lett.* 337–338, 144–155.
- Chen, C.-Y., Lee, J.-C., Chen, Y.-G., Chen, R.-F., 2014. Campaigned GPS on present-day crustal deformation in northernmost Longitudinal Valley preliminary results, Hualien Taiwan. *Terr. Atmos. Ocean. Sci.* 25, 337–357.
- Ching, K.-E., Hsieh, M.-L., Johnson, K.M., Chen, K.-H., Rau, R.-J., Yang, M., 2011. Modern vertical deformation rates and mountain building in Taiwan from precise leveling and continuous GPS observations, 2000–2008. *J. Geophys. Res.* 116, B08406. <http://dx.doi.org/10.1029/2011JB008242>.
- Davis, S.D., Frohlich, C., 1991. Single-link cluster analysis, synthetic earthquake catalogues, and aftershock identification. *Geophys. J. Int.* 104, 289–306.

- Hsieh, M.-L., Liew, P.-M., Hsu, M.-Y., 2004. Holocene tectonic uplift on the Hua-tung coast, eastern Taiwan. *Quat. Int.* 115–116, 47–70.
- Hsu, T.L., 1955. Earthquakes in Taiwan. *Quart. J. Bank Taiwan* 7 (2), 148–164 (in Chinese).
- Hsu, T.L., 1962. Recent faulting in the Longitudinal Valley of eastern Taiwan. *Mem. Geol. Soc. China* 1, 95–102.
- Huang, H.-H., Shyu, J.B.H., Wu, Y.-M., Chang, C.-H., Chen, Y.-G., 2012. Seismotectonics of northeastern Taiwan: Kinematics of the transition from waning collision to subduction and post-collisional extension. *J. Geophys. Res.* 117, B01313. <http://dx.doi.org/10.1029/2011JB008852>.
- Kobayashi, R., Nakanishi, I., 1994. Application of genetic algorithms to focal mechanism determination. *Geophys. Res. Lett.* 21, 729–732.
- Kuo Chen, H., Wu, Y.-M., Chang, C.-H., Hu, J.-C., Chen, W.-S., 2004. Relocation of the eastern Taiwan earthquakes and its tectonic implications. *Terr. Atmos. Ocean. Sci.* 15, 647–666.
- Lee, J.-C., Angelier, J., Chu, H.-T., Yu, S.-B., Hu, J.-C., 1998. Plate–boundary strain partitioning along the sinistral collision suture of the Philippine and Eurasian plates: Analysis of geodetic data and geological observation in southeastern Taiwan. *Tectonics* 17, 859–871.
- Lee, J.-C., Angelier, J., Chu, H.-T., Hu, J.-C., Jeng, F.-S., 2001. Continuous monitoring of an active fault in a plate suture zone: a creepmeter study of the Chihshang Fault, eastern Taiwan. *Tectonophysics* 333, 219–240.
- Lee, S.-J., Huang, H.-H., Shyu, J.B.H., Yeh, T.-Y., Lin, T.-C., 2014. Numerical earthquake model of the 31 October 2013 Ruisui, Taiwan, earthquake: Source rupture process and seismic wave propagation. *J. Asian Earth Sci.* 96, 374–385.
- Lee, T.T.-Y., Chan, C.-H., Shyu, J.B.H., Wu, Y.-M., Huang, H.-H., 2015. Induced transtensional earthquakes after the 1999 Chi-Chi earthquake in the compressional collision belt of western Taiwan. *Geophys. J. Int.* 200, 638–651.
- Liew, P.-M., Hsieh, M.-L., Lai, C.-K., 1990. Tectonic significance of Holocene marine terraces in the Coastal Range, eastern Taiwan. *Tectonophysics* 183, 121–127.
- Liu, C.-H., 1989. Sedimentological Research and Correlations of River Terraces Along the Liwu River M.S. thesis National Taiwan University (98 pp. in Chinese).
- Lu, C.-Y., Malavieille, J., 1994. Oblique convergence, indentation and rotation tectonic in the Taiwan mountain belt: insights from experimental modeling. *Earth Planet. Sci. Lett.* 121, 477–494.
- Shin, T.-C., 1992. Some implications of Taiwan tectonic features from the data collected by the Central Weather Bureau Seismic Network. *Meteorol. Bull.* 38, 23–48 (in Chinese).
- Shin, T.-C., 1993. Progress summary of the Taiwan strong motion instrumentation program. *Proceeding of Symposium on Taiwan Strong Motion Instrumentation Program, Central Weather Bureau, Taipei, Taiwan*, pp. 1–10 (in Chinese).
- Shyu, J.B.H., Sieh, K., Chen, Y.-G., 2005a. Tandem suturing and disarticulation of the Taiwan orogen revealed by its neotectonic elements. *Earth Planet. Sci. Lett.* 233, 167–177.
- Shyu, J.B.H., Sieh, K., Chen, Y.-G., Liu, C.-S., 2005b. Neotectonic architecture of Taiwan and its implications for future large earthquakes. *J. Geophys. Res.* 110, B08402. <http://dx.doi.org/10.1029/2004JB003251>.
- Shyu, J.B.H., Sieh, K., Avouac, J.-P., Chen, W.-S., Chen, Y.-G., 2006a. Millennial slip rate of the Longitudinal Valley fault from river terraces: Implications for convergence across the active suture of eastern Taiwan. *J. Geophys. Res.* 111, B08403. <http://dx.doi.org/10.1029/2005JB003971>.
- Shyu, J.B.H., Sieh, K., Chen, Y.-G., Chung, L.-H., 2006b. Geomorphic analysis of the Central Range fault, the second major active structure of the Longitudinal Valley suture, eastern Taiwan. *Geol. Soc. Am. Bull.* 118, 1447–1462.
- Shyu, J.B.H., Chung, L.-H., Chen, Y.-G., Lee, J.-C., Sieh, K., 2007. Re-evaluation of the surface ruptures of the November 1951 earthquake series in eastern Taiwan, and its neotectonic implications. *J. Asian Earth Sci.* 31, 317–331.
- Shyu, J.B.H., Sieh, K., Chen, Y.-G., Chuang, R.Y., Wang, Y., Chung, L.-H., 2008. Geomorphology of the southernmost Longitudinal Valley fault: Implications for evolution of the active suture of eastern Taiwan. *Tectonics* 27, TC1019. <http://dx.doi.org/10.1029/2006TC002060>.
- Shyu, J.B.H., Wu, Y.-M., Chang, C.-H., Huang, H.-H., 2011. Tectonic erosion and the removal of forearc lithosphere during arc–continent collision: Evidence from recent earthquake sequences and tomography results in eastern Taiwan. *J. Asian Earth Sci.* 42, 415–422.
- Teng, L.S., 1987. Stratigraphic records of the late Cenozoic Penglai orogeny of Taiwan. *Acta Geol. Taiwan.* 25, 205–224.
- Teng, L.S., 1990. Late Cenozoic arc–continent collision in Taiwan. *Tectonophysics* 183, 57–76.
- Wu, Y.-M., Chen, C.-C., 2007. Seismic reversal pattern for the 1999 Chi-Chi, Taiwan, Mw 7.6 earthquake. *Tectonophysics* 429, 125–132.
- Wu, Y.-M., Chiao, L.-Y., 2006. Seismic quiescence before the 1999 Chi-Chi, Taiwan, Mw 7.6 Earthquake. *Bull. Seismol. Soc. Am.* 96, 321–327.
- Wu, Y.-M., Chang, C.-H., Hsiao, N.-C., Wu, F.T., 2003. Relocation of the 1998 Ruyli, Taiwan, earthquake sequence using three-dimensions velocity structure with stations corrections. *Terr. Atmos. Ocean. Sci.* 14, 421–430.
- Wu, Y.-M., Chang, C.-H., Zhao, L., Shyu, J.B.H., Chen, Y.-G., Sieh, K., Avouac, J.-P., 2007. Seismic tomography of Taiwan: Improved constraints from a dense network of strong motion stations. *J. Geophys. Res.* 112, B08312. <http://dx.doi.org/10.1029/2007JB004983>.
- Wu, Y.-M., Chang, C.-H., Zhao, L., Teng, T.-L., Nakamura, M., 2008a. A comprehensive relocation of earthquakes in Taiwan from 1991 to 2005. *Bull. Seismol. Soc. Am.* 98, 1471–1481.
- Wu, Y.-M., Zhao, L., Chang, C.-H., Hsu, Y.-J., 2008b. Focal mechanism determination in Taiwan by genetic algorithm. *Bull. Seismol. Soc. Am.* 98, 651–661.
- Wu, Y.-M., Shyu, J.B.H., Chang, C.-H., Zhao, L., Nakamura, M., Hsu, S.-K., 2009a. Improved seismic tomography offshore northeastern Taiwan: Implications for subduction and collision processes between Taiwan and the southernmost Ryukyu. *Geophys. J. Int.* 178, 1042–1054.
- Wu, F.T., Liang, W.-T., Lee, J.-C., Benz, H., Villasenor, A., 2009b. A model for the termination of the Ryukyu subduction zone against Taiwan: A junction of collision, subduction/separation, and subduction boundaries. *J. Geophys. Res.* 114, B07404. <http://dx.doi.org/10.1029/2008JB005950>.
- Yamaguchi, M., Ota, Y., 2004. Tectonic interpretations of Holocene marine terraces, east coast of Coastal Range, Taiwan. *Quat. Int.* 115–116, 71–81.
- Yen, J.-Y., Lu, C.-H., Chang, C.-P., Hooper, A.J., Chang, Y.-H., Liang, W.-T., Chang, T.-Y., Lin, M.-S., Chen, K.-S., 2011. Investigating active deformation in the northern Longitudinal Valley and City of Hualien in eastern Taiwan using persistent scatterer and small-baseline SAR interferometry. *Terr. Atmos. Ocean. Sci.* 22, 291–304.
- York, J.E., 1976. Quaternary faulting in eastern Taiwan. *Bull. Geol. Surv. Taiwan* 25, 63–75.